Notable Features of Hybrid Modes in a Chiral-Filled Rectangular Waveguide

Abhay R. Samant and Keith W. Whites, *Member, IEEE*

***Abstract*—An analysis of hybrid modes in a rectangular waveguide filled with chiral material is presented in this paper. The modal wavenumbers are computed using the finite difference method together with Mullers root-finding algorithm. A novel scheme is presented whereby the validity of the numerical solution is established with analytical results. Using this numerical methodology, the existence of complex modes for a rectangular chiral waveguide is confirmed. Other notable features such as mode bifurcation and low frequency effects of chirality are also discussed.**

I. Solution Formulation and Verification

ELECTROMAGNETIC wave propagation in chiral material-filled guided wave structures, known as chiral waveguides, has only recently received attention in the literature [1]–[3]. In this paper, we will focus on the surprisingly complicated response of the rectangular chiral waveguide. Fig. 1 shows the geometry of this problem which is a longitudinally invariant waveguide filled with isotropic, homogenous, reciprocal chiral medium characterized by constant permittivity ϵ, permeability μ, and chirality parameter β through the Drude-Born-Federov constitutive equations

$$\overline{D} = \epsilon\overline{E} + \epsilon\beta\nabla \times \overline{E} \tag{1}$$

$$\overline{B} = \mu\overline{H} + \mu\beta\nabla \times \overline{H}. \tag{2}$$

The z-axis of the system of coordinates is taken parallel to the waveguide and we define the unit vectors $\hat{\tau}$, tangent to the curve C, and $\hat{n}$, normal to surface S, such that $\hat{\tau} \times \hat{n} = \hat{z}$.

As explained in [4], the phenomenon of wave propagation in a chiral-filled rectangular waveguide is governed by the following coupled set of partial differential equations (PDE's)

$$\nabla_t^2 E_z + (2\gamma^4\beta^2 + \gamma^2 - k_z^2)E_z - 2j\omega\beta\left(\frac{\gamma^4}{k^2}\right)\mu H_z = 0 \tag{3}$$

$$\nabla_t^2 H_z + (2\gamma^4\beta^2 + \gamma^2 - k_z^2)H_z + 2j\omega\beta\left(\frac{\gamma^4}{k^2}\right)\epsilon E_z = 0 \tag{4}$$

where an $e^{-jk_z z}$ dependence is assumed

$$\nabla_t^2 \equiv \frac{\partial^2}{\partial x^2} + \frac{\partial^2}{\partial y^2} \quad \text{and} \quad \gamma^2 = \frac{k^2}{1 - k^2\beta^2}$$

with $k = \omega\sqrt{\mu\epsilon}$.

Manuscript received November 11, 1994. This work was supported by the National Science Foundation Grant ECS-9210551.

A. R. Samant is with the Electromagnetic Communication Laboratory, University of Illinois, Urbana, IL 61801-2991 USA.

K. W. Whites is with the Department of Electrical Engineering, University of Kentucky, Lexington, KY 40506-0046 USA.

IEEE Log Number 9410017.

These PDE's are solved contingent upon the Dirichlet and generalized Neumann boundary conditions for the perfect electrically conducting walls

$$E_z|_S = 0 \tag{5}$$

$$\frac{\partial H_z}{\partial n}|_S = \alpha_1\frac{\partial}{\partial\tau}E_z + \alpha_2\frac{\partial}{\partial n}E_z + \alpha_3\frac{\partial}{\partial\tau}H_z \tag{6}$$

where

$$\alpha_1 = \frac{jk_z(\gamma_-^2 + \gamma_+^2)}{\alpha_4} \tag{7}$$

$$\alpha_2 = \frac{\gamma_+^2(k_z^2 + \gamma_-^2)^{1/2} - \gamma_-^2(k_z^2 + \gamma_+^2)^{1/2}}{\alpha_4} \tag{8}$$

$$\alpha_3 = \frac{k_z\eta(\gamma_-^2 - \gamma_+^2)}{\alpha_4} \tag{9}$$

$$\alpha_4 = -j\eta(\gamma_-^2(k_z^2 + \gamma_+^2)^{1/2} + \gamma_+^2(k_z^2 + \gamma_-^2)^{1/2}). \tag{10}$$

In (7)–(10), $\eta = \sqrt{\mu/\epsilon}$ and $\gamma_\pm^2 = k_\pm^2 - k_z^2$ where $k_\pm$ are, respectively, the wavenumbers for the right- and left-circularly polarized eigenwaves in an unbounded chiral medium

$$k_\pm = \frac{k}{1 \mp k\beta}. \tag{11}$$

Since it is difficult to obtain a simple analytical solution, a numerical approach based on the finite difference (FD) method is used to solve the coupled set of PDE's (3) and (4) with the associated boundary conditions (5) and (6) [4]. This leads to a set of equations which can be cast in the matrix form

$$\overline{\overline{Z}}(k_z) \cdot \overline{\Phi} = 0 \tag{12}$$

where $\overline{\Phi}$ is the vector of E_z and H_z coefficients at the nodes of the mesh within the appropriate solution space of each PDE. Muller's method [5] is then used to compute axial wavenumbers, k_z, which force the determinant of $\overline{\overline{Z}}$ to zero.

We have found that depending on the three initial guesses for Muller's method, these k_z roots can result in either a non-trivial or a trivial solution for $\overline{\Phi}$. Physically, the values of k_z for the trivial solution correspond to the right- and left-circularly polarized wavenumbers $k_\pm$ defined in (11). An analogous behavior can be observed both numerically and analytically for waveguides filled with simple materials where the trivial solutions degenerate to k, as does (11) when $\beta \to 0$.

While trivial solutions have little value in a physical setting, they can be a powerful tool in a numerical solution. As an illustration of this, Fig. 2 contains the plots of $k_\pm$ from (11) together with k_z roots found using our FD/Muller method outlined above. It is observed that the agreement between the

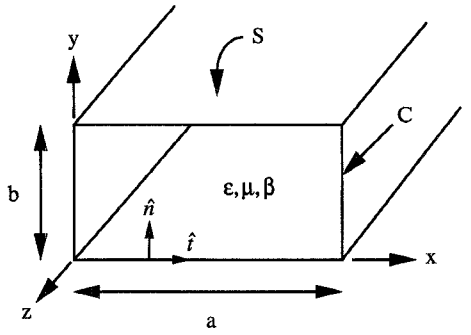

Fig. 1. Geometry of the rectangular chiral waveguide.

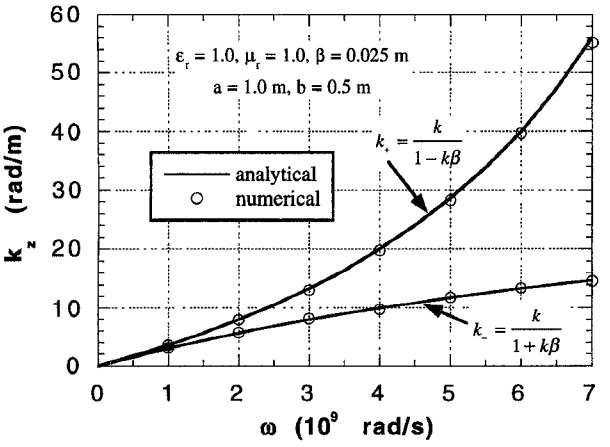

Fig. 2. Dispersion diagram for the two trivial solutions of the rectangular chiral waveguide having dimensions and constitutive parameters as shown.

two solutions is extremely close. While these k_z values would yield $\Phi = 0$ (a necessary consequence of the fact that the cutoff frequency for each mode is zero), in *toto* they are also a complete check of the numerical methodology. That is, these trivial solutions are a complete verification of the mathematical formulation, the boundary conditions and sufficiency of the mesh density used in the FD approach since all of these are constituents in the formation of $\overline{\overline{Z}}$ in (12)—whether the solution is trivial or not.

As an overview of the remainder of the paper, in Section II we will construct a k_z-β diagram for a set of chiral waveguide hybrid modes and subsequently confirm the existence of complex modes for the rectangular chiral waveguide. Finally in Section III we will study some significant features of the dispersion diagram for a set of hybrid modes.

II. Complex Modes

From the coupled set of PDE's (3) and (4) we see that the propagating modes in a chiral rectangular waveguide cannot be split into individual TE^z and TM^z modes and are hence referred to as hybrid modes. Using the mode tracing technique developed in [4], [6] we construct the k_z-β trace shown in Fig. 3. Based on the starting point at $\beta = 0$ and the mode nomenclature scheme given in [4], [6], the corresponding hybrid modes are labeled EH_{11} and HE_{11}.

An interesting feature of this graph is the region from $\beta \approx$ 0.08–0.131 m where no purely real nor purely imaginary solu-

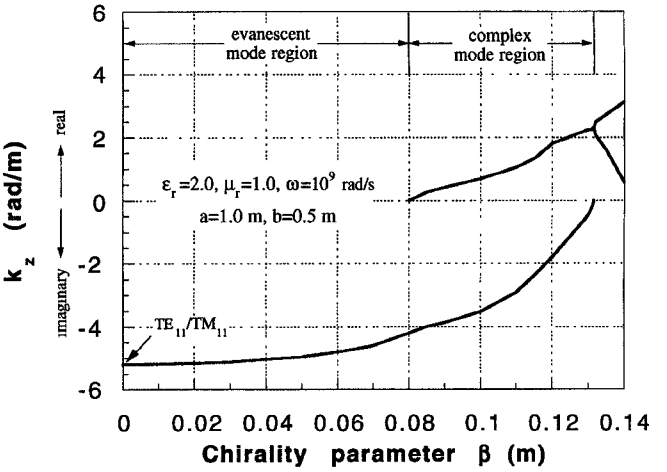

Fig. 3. $k_z - \beta$ diagram for the HE_{11}/EH_{11} hybrid modes of the rectangular chiral waveguide having dimensions and constitutive parameters as shown.

tion for k_z exists. The solutions instead are complex numbers and the modes corresponding to these values of k_z are known as complex modes. We have found that these modes exist in pairs having negative complex conjugate axial wavenumbers. This not only enforces the principle of conservation of energy [7] but also satisfies the necessary condition for these modes to physically exist in the problem [8]. (A detailed discussion on complex modes can be found in [9] and the references contained therein.)

The appearance of complex modes within a homogeneous, chiral waveguide has been observed elsewhere. In [10], these modes were observed in a circular chiral waveguide and in [11] for a square waveguide. However, in [11] a first-order perturbative solution technique was used and no validating results were shown. The data given in this paper serves to confirm the existence of complex modes in a rectangular chiral waveguide through the use of a complete numerical solution.

Two other distinct regions are apparent in Fig. 3; namely, an evanescent mode ($\beta < 0.08$ m) and a propagating mode ($\beta > 0.131$ m) region. Within this latter region (as well as the complex mode region), both the HE_{11} and EH_{11} modes have different axial wavenumbers. However, within the evanescent mode region these two hybrid modes apparently have degenerate k_z's. That is, for small values of β within the evanescent region, the numerical root searching procedure we used has not found more than one solution identifiable exclusively with the mode that is being traced. As β is increased, other roots may be detected but in all such instances we were able to ascribe these to dispersion curves associated with other hybrid modes.

III. Dispersion Diagrams

The dispersion graphs for the HE_{11} and EH_{11} chiral waveguide modes for two different nonzero values of chirality parameter are shown next in Fig. 4. Comparison with the non-chiral case shown in the figure indicates that the cutoff frequency is lowered by the introduction of chirality inside the waveguide. When the frequency is further increased beyond

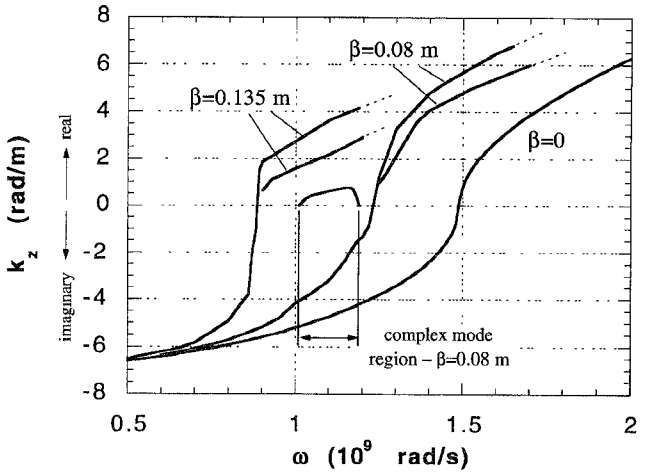

Fig. 4. Dispersion diagram for the HE_{11}/EH_{11} hybrid modes of the rectangular chiral waveguide (having dimensions and constitutive parameters as shown in Fig. 3) for three different β values.

cutoff, for each curve $\beta = 0.08$ and $\beta = 0.135$ m, we observe the appearance of two curves which apparently start from the same cutoff frequency but are split as the frequency increases. This phenomenon, defined as mode bifurcation, is one of the notable features of chiral waveguides and has been observed for parallel-plate [2] and circular [3] waveguides. As was the case in the previous section, the two hybrid modes apparently have degenerate k_z's within the evanescent mode region.

From Fig. 4, it is also interesting to note the dwindling effects of chirality on k_z at low values of frequency ($\omega \leq 0.5 \times 10^9$ rad/s). This phenomenon is expected and can be explained physically since for $\omega = 0$, $\nabla \times \overline{E} = 0$ which cancels the second term in (1) thereby nullifying the effects of chirality. It is important to note that this low frequency behavior is an intrinsic part of the constitutive equations (1) and (2) and is not dependent on the dispersive behavior of the constitutive parameters, contrary to other constitutive equations [12]. In particular, it can be shown that β is an even function of frequency and for chiral composite materials it has been found that β can be nonzero at dc [13].

IV. Conclusion

In this paper we have given examples of the relatively complicated response of the chiral rectangular waveguide as contrasted with those filled with simple materials. To establish the accuracy of the numerical methodology, we introduced a novel technique whereby the eigen-wavenumbers of the homogeneous chiral space are compared with the trivial numerical solutions for k_z of the waveguide. Some notable features of the HE_{11} and EH_{11} modes were presented which included the existence of complex modes, the phenomenon of mode bifurcation and the effects of chirality on k_z at low frequency.

References

[1] C. Eftimiu and L. W. Pearson, "Guided electromagnetic waves in chiral media," *Radio Sci.*, vol. 24, no. 3, pp. 351–359, 1989.
[2] P. Pelet and N. Engheta, "The theory of chirowaveguides," *IEEE Trans. Antenn. Propagat.*, vol. 38, no. 1, pp. 90–98, 1990.
[3] S. F. Mahmoud, "On mode bifurcation in chirowaveguides with perfect electric walls," *J. Electromagn. Waves Appl.*, vol. 6, no 10, pp. 1381–1392, 1992.
[4] A. R. Samant and K. W. Whites, "Electromagnetic wave propagation in a chiral-material-filled rectangular waveguide," *Microwave Opt. Technol. Lett.*, vol. 8, no. 2, pp 106–111, Feb. 5, 1995
[5] W. H. Press, S. A. Teukolsky, W. T. Vetterling, and B. P. Flannery, *Numerical Recipes in FORTRAN*, 2nd ed. Cambridge, MA: Cambridge University Press, 1992.
[6] A. R. Samant, "Electromagnetic wave propagation in a chiral-filled rectangular waveguide," M. S. thesis, Univ. of Kentucky, 1994.
[7] P. Chorney, "Power and energy relations in bidirectional waveguides," Mass Inst. Tech. Res. Lab of Electronics, Tech. Rep 396, Sept., 1961.
[8] S. R. Laxpati and R. Mittra, "Energy considerations in open and closed waveguides," *IEEE Trans. Antenn. Propagat.*, vol. AP-13, no. 6, pp. 883–890, 1965.
[9] K W Whites and R Mittra, "Complex and backward-wave modes in dielectrically loaded lossy circular waveguides," *Microwave Opt. Technol. Lett.*, vol. 2, no. 6, pp. 199–204, 1989.
[10] G. Busse and A. F. Jacob, "Complex modes in circular chirowaveguides," *Electron. Lett.*, vol. 29, no. 8, pp 711–713, 1993.
[11] H. Cory, "Wave propagation along a closed rectangular chirowaveguide," *Microwave Opt. Technol. Lett.*, vol. 6, no 14, pp. 797–800, 1993.
[12] I. V. Lindell, A. H. Sihvola, S. A. Tretyakov, and A. J. Viitanen, *Electromagnetic Waves in Chiral and Bi-Isotropic Media.* Boston: Artech House, 1994.
[13] K. W. Whites, "Full-wave computation of constitutive parameters for lossless composite chiral materials," to be published in *IEEE Trans. Antenna Propagat*